Title
Wave-particle decorrelation and transport of anisotropic turbulence in collisionless plasmas.

Journal
Physical review letters, 99(26)

ISSN
0031-9007

Authors
Lin, Z
Holod, I
Chen, L
et al.

Publication Date
2007-12-01

DOI
10.1103/physrevlett.99.265003

Peer reviewed

Wave-Particle Decorrelation and Transport of Anisotropic Turbulence in Collisionless Plasmas

Z. Lin,* I. Holod, and L. Chen
Department of Physics and Astronomy, University of California, Irvine, California 92697, USA

P. H. Diamond
Department of Physics, University of California, San Diego, California 92093, USA

T. S. Hahm and S. Ethier
Princeton Plasma Physics Laboratory, Princeton University, Princeton, New Jersey 08543, USA
(Received 2 August 2007; published 27 December 2007)

Comprehensive analysis of the largest first-principles simulations to date shows that stochastic wave-particle decorrelation is the dominant mechanism responsible for electron heat transport driven by electron temperature gradient turbulence with extended radial streamers. The transport is proportional to the local fluctuation intensity, and phase-space island overlap leads to a diffusive process with a time scale comparable to the wave-particle decorrelation time, determined by the fluctuation spectral width. This kinetic time scale is much shorter than the fluid time scale of eddy mixing.

DOI: 10.1103/PhysRevLett.99.265003 PACS numbers: 52.35.Ra, 52.25.Fi, 52.35.Kt, 52.65.−y

Turbulence of the fusion plasma in a tokamak reactor, where magnetic field lines form nested flux surfaces to confine charged particles, is often excited by pressure-gradient-driven, electrostatic, drift-wave instabilities [1] possessing anisotropic mode structures. Turbulence eddies rotate along surfaces of constant electrostatic potentials in the direction perpendicular to both the electric and magnetic fields ($E \times B$ drift). In the prevailing fluid picture [2], transport is understood as arising from the eddy mixing process of a random walk with a correlation length of the eddy size and with a decorrelation time of the eddy turnover time [3,4]. The mixing length argument [5] conjectures that transport increases sensitively with the eddy size along the radial direction of pressure gradients.

The concept of turbulent transport via the eddy mixing is valid when the collisional mean-free-path of constituent particles is much shorter than the eddy correlation length so that particles and eddies move together as fluid elements. However, in high temperature fusion plasmas, the mean-free-path of charged particles along the magnetic field lines is much longer than typical eddy length in the parallel direction. In this nearly collisionless, wave-dominated plasma turbulence, transport in the radial direction is supported by the random $E \times B$ motions of charged particles. If charged particles decouple from turbulence eddies due to kinetic effects before eddies could execute a complete rotation, the transport process is regulated by the kinetic wave-particle decorrelation rather than by the fluid eddy mixing.

We report here the first results from the largest ever plasma simulations that wave-particle decorrelation is the dominant mechanism responsible for the electron heat transport driven by electron temperature gradient (ETG) turbulence [6]. As a paradigm of anisotropic turbulence, ETG turbulence is dominated by elongated eddies (streamers) and is a subject of current interest as a candidate for driving electron heat transport in fusion plasmas [7–14]. Various spatial and temporal scales of the ETG turbulence are calculated through comprehensive analysis of the massive data produced from our simulations. We find that ETG transport is proportional to the local fluctuation intensity, and that phase-space island overlap leads to a diffusive process with a time scale comparable to the wave-particle decorrelation time determined by the fluctuation spectral width. This kinetic time scale is much shorter than the fluid time scale of eddy mixing. Therefore, transport in the ETG turbulence is in the low Kubo number regime. Since the ratio of fluid-to-kinetic time scales increases with the device size, the extrapolation of the transport level from present-day experiments to future larger reactors could be overly pessimistic, if we invoke the simplistic mixing length argument with the streamer length as the spatial step size and the fluid time scale as the time step size.

ETG simulation.—The ETG turbulence in a tokamak is studied using gyrokinetic particle-in-cell simulations [15], which suppress the rapid gyromotion of charged particles about magnetic field lines to remove high frequency modes and to reduce the dimension of phase space from six to five. Both linear and nonlinear wave-particle interactions, and nonlocal geometric effects are treated rigorously in a well-benchmarked, massively parallel, global gyrokinetic toroidal code (GTC) [4]. A global field-aligned mesh [16] provides the maximal computational efficiency without any approximation in physics or geometry to describe the toroidal drift-wave eigenmode [17] with anisotropic structures. An effective collision operator modeling a heat bath [18] prevents the relaxation of temperature profile. Ion response is adiabatic since the ETG wavelength is much smaller than the ion gyroradius. The tokamak with concentric flux surfaces is described by magnetic coordinates

(r, θ, ζ), where r is the radial coordinate labeling the flux surfaces, θ is the poloidal angle, and ζ is the toroidal angle. Global GTC simulations use representative tokamak plasmas with the following local parameters at a radial position $r = 0.5a$, $R/L_T = 5.3$, $R/L_n = 2.2$, $q = 1.4$, $s = 0.78$, $T_e/T_i = 1$, and $a/R = 0.36$. Here R is the major radius, a is the minor radius, L_T and L_n are the electron temperature and density gradient scale lengths, T_i and T_e are the ion and electron temperatures, q is the safety factor, and s is the magnetic shear. The boundary condition of the perturbed electrostatic potential $\phi = 0$ is enforced at $r < 0.1a$ and $r > 0.9a$. The size of the tokamak used in the simulation is $a = 500\rho_e$, where $\rho_e = v_e/\Omega_e$ is electron gyroradius with electron cyclotron frequency Ω_e, electron thermal speed $v_e = (T_e/m_e)^{1/2}$, and electron mass m_e. The computational mesh consists of 32 toroidal grids, and a set of unstructured radial and poloidal grids with a perpendicular grid size of ρ_e. The time step is $0.2L_T/v_e$. The ETG mode is unstable with a linear threshold of $R/L_T = 4$, and the most unstable linear mode centers at $r = 0.5a$ with a poloidal wave vector $k_\theta\rho_e = 0.35$, a real frequency $\omega = 0.12v_e/L_T$, and a growth rate $\gamma = 0.030v_e/L_T$.

The simulation starts with random perturbations of small amplitude. The unstable ETG modes first grow exponentially, as evident in the electron heat conductivity χ_e shown in Fig. 1, then saturate at time $t \approx 430L_T/v_e$, and finally evolve into turbulence with steady state transport. Here, the heat conductivity $\chi_e = QL_T/T_e$ is calculated using the heat flux $Q = \int \frac{1}{2} m_e v^2 \delta v_r \delta f d^3 v$ measured from simulations, where v is the electron velocity, δv_r is the radial $E \times B$ drift, and δf is the perturbed distribution function. The particle flux is zero because of the ion adiabatic response and quasineutrality condition. Numerical convergence with respect to grid size and time step have been achieved by varying the grid size and the time step. More importantly, convergence with respect to the number of particles needs to be carefully studied to make sure that numerical noise [15] associated with discreteness in the phase space does not affect the physics being studied. In Fig. 1, it is shown that transport level (and other statistically significant quantities such as fluctuation intensity) changes little when the number of particles per cell increases from 400 to 2000. To further quantify the effects of the particle noise in ETG simulations, the noise-driven transport is measured directly using a scramble test, calculated by a quasilinear theory using the noise spectrum measured in simulations, and estimated using the entropy [19]; all agree within a factor of 2. In Fig. 1, the estimated noise-driven transport is shown to be 4000 times smaller than the ETG turbulent transport in the simulation using 2000 particles per cell. This definitive demonstration of convergence with respect to the number of particles in simulations on the long time scales has only recently become feasible thanks to the newly available computing resources that enable these simulations with 38×10^9 particles and ten thousand time steps by using 70 hours of 6400 processors of a Cray supercomputer.

Nonlinear saturation.—This numerically-converged, long-time simulation achieving steady state turbulence provides a solid basis for studying ETG nonlinear saturation and transport mechanism. In the linear phase, ETG toroidal eigenmodes form with an average parallel component of wave vector $\bar{k}_{||}R \approx 0.9$, and an average poloidal component of wavevector $\bar{k}_\theta\rho_e \approx 0.26$, as shown in the early time of Fig. 2. The initial nonlinear saturation of the ETG instability is primarily due to nonlinear toroidal mode coupling, consistent with theoretical analysis [11,12]. The spectral energy gradually flows towards longer wavelengths, eventually down to damped modes, as indicated by the downshift of the poloidal spectrum to $\bar{k}_\theta\rho_e \approx 0.18$. The width of the poloidal spectrum increases to $\Delta k_\theta\rho_e \approx 0.08$. The parallel spectrum also increases to $\bar{k}_{||}R \approx 1.0$ in the steady state. On a longer time scale, the spatial re-

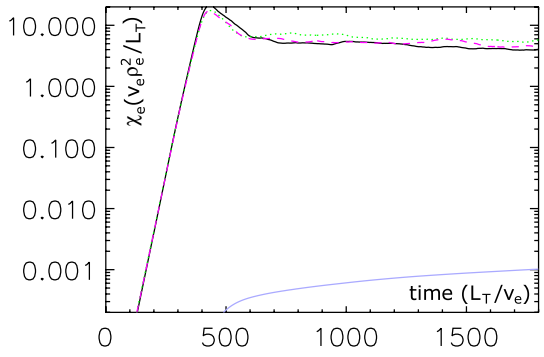

FIG. 1 (color online). Time history of electron heat conductivity. The upper three curves are χ_e driven by the ETG turbulence with a number of particles per cell 2000 (solid black), 1000 (dotted green), and 400 (dashed red). The lower curve (solid blue) is χ_e driven by particle noise for the case of 2000 particles per cell. χ_e is averaged over a radial domain of $r/\rho_e = [200, 300]$.

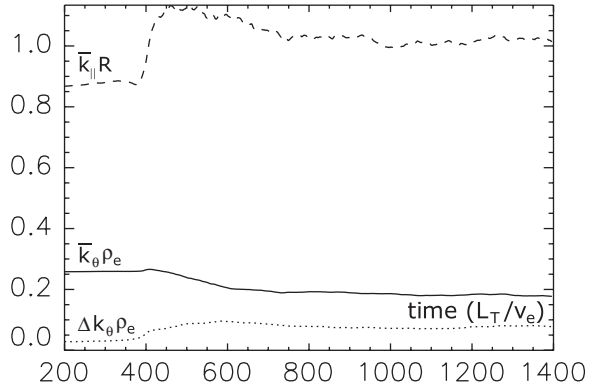

FIG. 2. Time history of parallel wave vector $\bar{k}_{||} = \sqrt{\langle k_{||}^2\phi^2\rangle/\langle\phi^2\rangle}$ (dashed), poloidal wave vector $\bar{k}_\theta = \sqrt{\langle k_\theta^2\phi^2\rangle/\langle\phi^2\rangle}$ (solid), and spectral width $\Delta k_\theta = \sqrt{\langle(k_\theta - \bar{k}_\theta)^2\phi^2\rangle/\langle\phi^2\rangle}$ (dotted) for electrostatic potential ϕ at $r/\rho_e = [238, 262]$.

arrangement of fluctuations occurs via turbulence spreading in which fluctuation energy flows from unstable to stable radial regions [16,18]. The steady state is maintained through the balance of sources and sinks in both spectral and real spaces.

The structures of electrostatic potential in steady state ETG turbulence are shown in Fig. 3. The apparently coherent structures actually consist of many ($\sim 10^2$) unstable toroidal eigenmodes with significant amplitudes. Each eigenmode with a toroidal mode number n contains many poloidal m harmonics. Each m harmonic has a narrow radial width centered around its mode rational surface r_0, where $q(r_0) = m/n$. For modest positive magnetic shear, neighboring m harmonics overlap to form radially elongated structures, i.e., macroscopic streamers with a radial scale close to the temperature gradient length L_T. During the saturation process [11], generation of zonal flows ($n = m = 0$ harmonics) is too weak to break up the radial streamers or to affect the electron transport (thus zonal flows are not included in subsequent analysis). This is in contrast to the ion temperature gradient (ITG) turbulence where strong zonal flows break up the streamers [4]. Note that when magnetic shear s is negative or weak, ETG turbulence is not dominated by streamers [8] and the transport is low. To estimate the streamer length, we calculate the two-point correlation function, $C_{r\zeta}(\Delta r, \Delta\zeta) = \frac{\langle\phi(r+\Delta r,\zeta+\Delta\zeta)\phi(r,\zeta)\rangle}{\sqrt{\langle\phi^2(r+\Delta r,\zeta+\Delta\zeta)\rangle\langle\phi^2(r,\zeta)\rangle}}$, where $\langle\cdots\rangle$ represents averaging over $\zeta = [0, 2\pi]$ and $r/\rho_e = [200, 350]$ at $\theta = 0$. Radial correlation function $C_r(\Delta r)$ is then calculated by taking the maximal value along the ridge of $C_{r\zeta}(\Delta r, \Delta\zeta)$. The function $C_r(\Delta r)$ decays exponentially for small radial separation $\Delta r < 40\rho_e$, but possesses a significant tail because of the streamers. The radial correlation length, defined as $L_r = \frac{\langle \Delta r C_r\rangle}{\langle C_r\rangle}$, is found to be $L_r \approx 54\rho_e$. Note that this is an underestimation of the streamer length since streamers are not oriented in parallel. The poloidal correlation length is found to be $L_\theta \approx 7\rho_e$. For comparison, the average distance between all rational surfaces of unstable modes is $d_r = r/(sqn^2) \sim 0.22\rho_e$ using $n \sim 32$ for $\bar{k}_\theta\rho_e \approx 0.18$.

Transport mechanism.—The presence of radial streamers has been conjectured to drive large heat transport based on the commonly invoked mixing length argument of a transport mechanism of eddy diffusion with a step size corresponding to the eddy radial size (L_r) and a time step of the linear growth time ($1/\gamma$). However, such estimate of the streamer transport would yield an electron heat conductivity χ_e an order of magnitude higher than the value measured in simulations. To resolve this discrepancy, we examine the dependence of transport on fluctuation intensity, which is responsible for electron radial heat flows. It is shown in Fig. 4 that the electron heat conductivity χ_e is proportional to the local fluctuation intensity $|\delta v_r|^2$ of the fluctuating radial $E \times B$ drift. The fact that transport is proportional to the local fluctuation intensity suggests a diffusive process relevant to the weak turbulence regime. In contrast, transport is proportional to fluctuation amplitude $|\delta v_r|$ in the strong turbulence regime, where the decorrelation process is regulated by the coherent wave trapping of particles or by eddy self-interaction.

Using the quasilinear estimate, a phenomenological wave-particle decorrelation time can be defined as $\tau_{\rm wp} = \frac{2D}{\delta v_r^2} \approx 4.3 L_T/v_e$, where $D = 2\chi_e/3$ is assumed. The effective radial step size is $\Delta r = \tau_{\rm wp}\delta v_r \approx 5.6\rho_e$. The fact that $d_r \ll \Delta r \ll L_r$ is consistent with observations from ETG simulations that electrons do not rotate around the full radial extent of streamers [11,13], and further supports the picture of diffusive process resulting from overlap of phase-space islands in the presence of densely packed mode rational surfaces. Consistently, $\tau_{\rm wp}$ is found to be comparable to the wave-particle decorrelation time associated with the collisionless parallel motion of electrons. The parallel decorrelation time due to the parallel dispersion and set by the spectral width of the parallel wave vector ($\Delta k_\parallel \approx \bar{k}_\parallel$) is $\tau_\parallel = \frac{1}{\Delta k_\parallel v_e} \approx 5.3 L_T/v_e$. Another kinetic effect is resonance broadening [20], induced by the radial particle diffusion. The time scale for electron diffu-

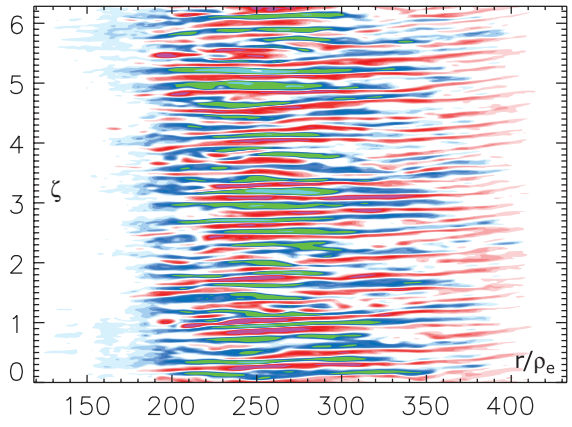

FIG. 3 (color). Contour plot of electrostatic potential $\phi(r, \zeta)$ at $\theta = 0$ and $t = 1400 L_T/v_e$. Pink and red represent positive value; blue and green represent negative value.

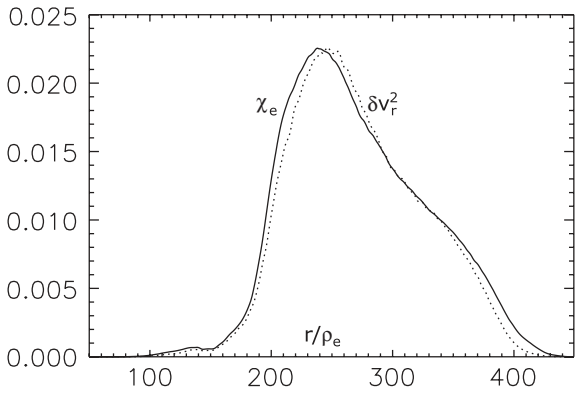

FIG. 4. Radial profile of χ_e and δv_r^2. Solid line is $\chi_e(\nu_e\rho_e)$ and dotted line is $\delta v_r^2(\nu_e^2)$ multiplied by 825, both are flux-surface and time averaged for $t = [800, 1400] L_T/v_e$.

TABLE I. Time scales in units of L_T/ν_e for ETG turbulence.

$\tau_{\rm wp} = \frac{4\chi_e}{3\delta\nu_r^2}$	$\tau_{\|\|} = \frac{1}{\Delta k_{\|\|}\nu_e}$	$\tau_\perp = \frac{3}{4s^2\bar{\theta}^2\bar{k}_\theta^2\chi_e}$	$\tau_{\rm eddy} = \frac{L_r}{\delta\nu_r}$	$\tau_{\rm rb} = \frac{4L_r^2}{3\chi_e}$	$\tau_{\rm auto}$	$\frac{1}{\gamma}$
4.2	5.3	8.0	42	437	346	33

sions across the radial structure of a poloidal m harmonic is $\tau_\perp = \frac{3}{4s^2\bar{\theta}^2\bar{k}_\theta^2\chi_e} \approx 8.0 L_T/\nu_e$. Here, the radial wave vector k_r of the m harmonics is related to the parallel mode width θ through $k_r = s\theta k_\theta$ with $\bar{\theta}^2 = \frac{\langle\theta^2\phi^2\rangle}{\langle\phi^2\rangle} \approx 0.95$. On the other hand, the time scale for electron diffusion across the radial streamers is $\tau_{\rm rb} = \frac{3L_r^2}{4\chi_e} \approx 437 L_T/\nu_e$. The fact that $\tau_{\rm wp} \approx \tau_{\|\|} \leq \tau_\perp \ll \tau_{\rm rb}$ shows that the transport process is dominated by the wave-particle decorrelation controlled by the parallel motion and the parallel spectral width. The decorrelation due to the radial localization of the m harmonics is also relevant, although subdominant. On the other hand, the streamer length is not directly related to the transport process, i.e., particle stochasticity, rather than eddy mixing, controls the transport.

To confirm the kinetic origin of electron heat transport, kinetic time scales must be shorter than the fluid mode-coupling energy transfer time. The eddy turnover time is $\tau_{\rm eddy} = \frac{L_r}{\delta\nu_r} \approx 42 L_T/\nu_e$. Since the ETG eigenmodes shown in Fig. 3 propagate along the toroidal direction with fixed phase velocities, the Lagrangian decorrelation time is the relevant decorrelation time scale. The two-spatial-point, two-time correlation function for the electrostatic potential is defined as $C_{t\zeta}(\Delta t, \Delta\zeta) = \frac{\langle\phi(t+\Delta t,\zeta+\Delta\zeta)\phi(t,\zeta)\rangle}{\sqrt{\langle\phi^2(t+\Delta t,\zeta+\Delta\zeta)\rangle\langle\phi^2(t,\zeta)\rangle}}$, where potential data are taken at $r = 0.5a$ and $\theta = 0$ and $\langle\cdots\rangle$ represents an average over $\zeta = [0, 2\pi]$ and for $t = [600, 1400] L_T/\nu_e$. The slope of dominant structures of $C_{t\zeta}(\Delta t, \Delta\zeta)$ represents average toroidal phase velocity $\nu_\zeta \approx 0.0018$ rad ν_e/L_T, which corresponds to a poloidal phase velocity of $\nu_\theta \approx 0.32\nu_e\rho_e/L_T$ for field-aligned modes. This measured ν_θ is close to the linear phase velocity $\omega/k_\theta \approx 0.34\nu_e\rho_e/L_T$ of the ETG modes, suggestive of wave-dominated turbulence. Now we calculate the Lagrangian time correlation function by taking the maximal value along the ridge of $C_{t\zeta}(\Delta t, \Delta\zeta)$, i.e., moving with the wave phase velocity. The Lagrangian correlation function $C_t(\Delta t)$ decays exponentially with an autocorrelation time $\tau_{\rm auto} \approx 346 L_T/\nu_e$. Thus, we show that the fluid time scales are 2 orders of magnitude longer that the wave-particle decorrelation time.

Relevant time scales in ETG turbulence are summarized in Table I. Since $\tau_{\rm wp} \approx \tau_{\|\|}$, $\tau_\perp \ll \tau_{\rm eddy}$, $\tau_{\rm rb}$, $\tau_{\rm auto}$ we conclude that wave-particle decorrelation is the dominant mechanism for electron heat transport driven by the toroidal ETG turbulence, and that the transport level can be calculated using the quasilinear theory. The quasilinear expression [5] for the test particle diffusion coefficient [19] is $D(\mathbf{v}) = \frac{\pi c^2}{B^2}\int\frac{d\mathbf{k}}{(2\pi)^3}\int\frac{d\omega}{2\pi}\times\langle|\phi^2|\rangle_{\omega\mathbf{k}} k_\theta^2 J_0^2(k_\perp\rho)\delta(k_{\|\|}\nu_{\|\|} - \omega)$, where B is the magnetic field and J_0 is the Bessel function. The spectrum is constructed for potential data at $r = 0.5a$ and $t = 1400 L_T/\nu_e$, using the linear dispersion relation $\omega = k_\theta\nu_\theta$ and assuming an infinite radial correlation length. The quasilinear value for the heat conductivity $\chi_{\rm ql} = \frac{3}{2}\int d^3\mathbf{v} D(\mathbf{v}) f_M(\mathbf{v}) \approx 6.1\rho_e\nu_e^2/L_T$ is in good agreement with the value of χ_e measured from simulations (f_M is the Maxwellian distribution function). Therefore, ETG transport is driven by the local fluctuation intensity through a particle diffusion process, although ETG turbulence intensity and spectral properties are determined predominantly by wave-wave couplings, which can be treated approximately by fluid equations [11,12].

This work was supported by U.S. DOE Grants No. DE-FG02-07ER54916, No. DE-FC02-04ER54796, and No. DE-FG03-94ER54736 (UCI), and in part by No. DE-FG02-04ER54738 (UCSD) and No. DE-AC02-CHO-3073 (PPPL). Simulations used ORNL supercomputers. Z. L. gratefully acknowledges Scott Klasky for computational support and Fulvio Zonca for useful discussions.

*zhihongl@uci.edu

[1] W. Horton, Rev. Mod. Phys. **71**, 735 (1999).
[2] A. Hasegawa and K. Mima, Phys. Fluids **21**, 87 (1978).
[3] H. Biglari, P. H. Diamond, and P. W. Terry, Phys. Fluids B **2**, 1 (1990).
[4] Z. Lin *et al.*, Science **281**, 1835 (1998).
[5] B. B. Kadomtsev, *Plasma Turbulence* (Academic, London, 1965).
[6] W. Horton, B. G. Hong, and W. M. Tang, Phys. Fluids **31**, 2971 (1988).
[7] F. Jenko *et al.*, Phys. Plasmas **7**, 1904 (2000).
[8] Y. Idomura, M. Wakatani, and S. Tokuda, Phys. Plasmas **7**, 3551 (2000).
[9] B. Labit and M. Ottaviani, Phys. Plasmas **10**, 126 (2003).
[10] J. Q. Li and Y. Kishimoto, Phys. Plasmas **11**, 1493 (2004).
[11] Z. Lin, L. Chen, and F. Zonca, Phys. Plasmas **12**, 056125 (2005).
[12] L. Chen, F. Zonca, and Z. Lin, Plasma Phys. Controlled Fusion **47**, B71 (2005).
[13] N. Joiner *et al.*, Plasma Phys. Controlled Fusion **48**, 685 (2006).
[14] R. E. Waltz, J. Candy, and M. Fahey, Phys. Plasmas **14**, 056116 (2007).
[15] W. W. Lee, J. Comput. Phys. **72**, 243 (1987).
[16] Z. Lin *et al.*, Phys. Rev. Lett. **88**, 195004 (2002).
[17] F. Romanelli and F. Zonca, Phys. Fluids B **5**, 4081 (1993).
[18] Z. Lin and T. S. Hahm, Phys. Plasmas **11**, 1099 (2004).
[19] I. Holod and Z. Lin, Phys. Plasmas **14**, 032306 (2007).
[20] T. H. Dupree, Phys. Fluids **11**, 2680 (1968).